Article:
Lanigan, JL, Fatima, S, Charpentier, TV orcid.org/0000-0002-3433-3511 et al. (3 more authors) (2018) Lubricious ionic polymer brush functionalised silicone elastomer surfaces. Biotribology, 16. pp. 1-9.

https://doi.org/10.1016/j.biotri.2018.08.001

Lubricious ionic polymer brush functionalised silicone elastomer surfaces

J. L. Lanigan, S. Fatima, T. V. Charpentier, A. Neville, D. Dowson, **M. Bryant***

Institute of Functional Surfaces (iFS), School of Mechanical Engineering, University of Leeds, United Kingdom, LS2 9JT

Corresponding Author: m.g.bryant@leeds.ac.uk

ABSTRACT

Infection, erosion of mucosal and uro-epithelial layers, tissue trauma and encrustation associated with catheterisation is still an issue faced by health-care professionals and patients – effecting patients subject to spinal cord injuries, chemotherapy and incontinence to name a few. Over the past decade efforts have been made to optimise catheter surfaces in an attempt to reduce the occurrence of trauma related complications during insertion. Organic and inorganic materials have been mooted as potential methods of reducing bio-film formation and increasing lubricity. The use of charged species has been further hypothesised as a potential method to reduce the occurrence of bio-film formation, reducing the need for therapeutic intervention. This study investigates the feasibility of functionalising silicone surfaces with charged ionic polymer brush technologies with the view to reduce urethral trauma and infection for indwelling and self-catheterisation devices. A simple three step synthesis route has been proposed, complimented by surface analysis and tribological assessment of the surfaces. The effects of initial monomer content on the functional outcomes of the surfaces has been investigated. Functionalisation of surfaces was seen to significantly reduce the hydrophobicity of the surfaces. A significant reduction in the coefficient of friction from $\mu = 0.4$ to 0.005 for un-functionalised and functionalised surfaces, respectively, was seen. The speed dependence and effects of lubricant chemistry on the coefficient of friction have also been investigated.

KEYWORDS: Urinary Incontinence; Catheters; Polymer Brush; Aqueous Lubrication

1. Introduction

Since the 1940's, silicones and other hydrophobic elastomers such as poly vinyl chloride and polyurethanes, have found extensive use in healthcare due to their bio-compatibility, mechanical properties and durability [1]. Silicones are now ubiquitous in medicine and are used for implantable devices such as catheters, drains, shunts and prosthetics as well as extracorporeal equipment, due to their hemocompatibility and permeability properties. The use of silicone catheters is wide-spread for the management of urine out of the bladder. This typically involves the insertion of a silicone tube into the urethra or lower stomach (Suprapubic), bypassing the urinary sphincter and into the bladder. A balloon is then inflated within the bladder allowing urine to flow through the catheter into a collection bag. The design and use of materials for urinary catheterisation has remained relatively unchanged since their inception. Pain during insertion, infection, erosion of epithelial layers, tissue trauma and encrustation are still common and represent a significant burden on the health services [2]. Without doubt, a functional device-biology interface is key if successful intermittent and in-dwelling medical devices are to be achieved.

Despite its widespread use, the inherent hydrophobicity of the silicone surface makes it undesirable from a tribological point of view. Values of coefficient of friction (μ) are regularly quoted and range from 0.1 to 0.5 for un-functionalised silicone surfaces against a wide range of counter-body materials [3, 4]. Over the past decade efforts have been made to optimise silicone surfaces in an attempt to reduce friction and reduce/eliminate infection and encrustation [5]. Organic and inorganic materials have been mooted as potential strategies to reducing bio-film formation and increase lubricity. Hydrogel coatings (i.e. networks of crosslinked polymer chains in an aqueous solvent) are available and have been shown to be effective in reducing biofilm formation, trauma and encrustation due to their hydrophilic nature [6, 7]. These are often user applied with no direct bonding to the surface and, as such, questions are raised regarding their durability.

Polymer brush surfaces consist of a layer of bio-inspired polymers with one end chemically grafted to the surface [8]. Such surfaces are inspired from the bio-macromolecules observed in nature replicating the highly hydrated regions of proteoglycans and phospholipid membranes [9]. The application of polymer brush technologies has received much attention by researchers over the past decade as an interesting class of thin-film polymer surfaces. Many investigators have shown the ability to tailor a surface, in terms of fouling and friction, through selective grafting or polymer chemistry [2]. From a biomedical and surface engineering point of view, charged polymers are becoming of particular interest because of their bio-compatibility, low-fouling and ability to impart low coefficients of friction

[2, 8, 9]. Such surfaces are attractive for application such as catheterisation, drug delivery and modification of elastomer prosthetic surfaces [10, 11].

This study aims to develop a simple method for the functionalisation of silicone surfaces with anionic polymer brush technologies. The grafting of charged polymers to a surface aims to exploit the biological environment for enhanced lubrication, but also provide surfaces with enhanced anti-fouling capabilities as seen in other areas of bio-fouling. This study presents a simple functionalisation method and systematically investigates the roles of synthesis parameters on the lubrication properties of the surfaces under a wide range of loads and sliding speeds. In the long term, the produced surfaces will be capable of reducing tissue trauma and infection for indwelling and self-catheterisation devices.

2. Materials and Methodology

2.1. Materials and Reagents

3-Sulfopropyl methacrylate potassium salt (SPMK) was purchased from Sigma Aldrich and used as received. SPMK was dissolved in de-ionised water at three concentrations; 5, 10 and 20 wt%. Polydimethylsiloxane (PDMS) was used as an idealised material. Samples were prepared using a Sylgard 184 elastomer kit (Dow-Corning, USA). The PDMS kit was mixed at a ratio of 10:1 (by weight) and poured into polystyrene moulds facilitating the production of a 4mm thick silicone slab (E = 1.8 – 2 MPa, measured in our lab). The mixtures were transferred into the mould after removing bubbles under vacuum and then incubated in an oven (70 °C) for 24 hours. Samples were then cut from the slabs (Ø 5 x 4 mm) and used as the substrate material in this study.

2.2. Surface Synthesis

Figure 1 shows the steps involved in grafting surfaces with SPMK. The ‘as cast’ and ‘cut’ PDMS surfaces were cleaned using in an O-Zone plasma chamber for 60 seconds (50 W at 60 mTorr). Surfaces were removed and immediately placed in a 12 well cell culture plate within a N_2 glove box. These were then immersed in the monomer solution (M_i, 5, 10 & 20 wt% in de-ionised water) which had been degassed with N_2 for at least 30 mins. Polymerisation was then initiated by UV irradiation for 3 hrs at 60 °C (365 nm at 5 mW/cm^2). After polymerisation, surfaces were removed and rinsed with de-ionised water for 30 minutes, followed by drying with an N_2 air stream. Surfaces were then stored dry prior to testing.

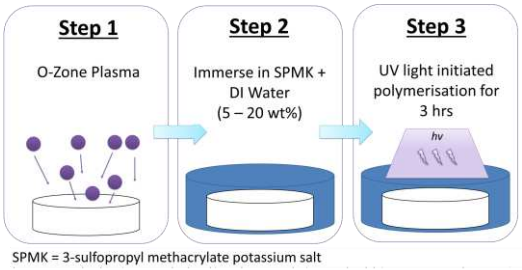

(a)

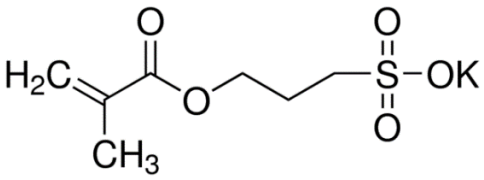

(b)

Figure 1 – a) Schematic representation of the three-step process for creating PDMS-g-SPMK surfaces and b) monomer used in this study.

To determine the average molecular weight (M_n) of the polymers after UV exposure, residual polymer solution was removed prior to the surfaces been rinsed with DI water. The viscosity of the residual polymer solution after UV exposure was measured at five different dilutions in DI water. An m-VROC (RheoSense, USA) micro-fluidic, micro-electrical mechanical based viscometer was used to determine the viscosity of the solution at a flow rate of 600 µL / minute. The intrinsic viscosity [η] for the solution was determined and related to molecular weight using the Mark-Houwink-Sakurada relationship. Where K and α are constants, assumed to be 2.06 x 10^{-3} mL/mg and 0.5 respectively [12].

Eq1:
$$[\eta] = KM_n^{\alpha}$$

2.3. Surface Characterisation

Static contact angle (CA) was acquired at ambient temperature (25 °C). A droplet of 5 µL of deionized water was used as probe liquid. Five different positions were measured for each sample to get the average CA. All the contact angles were measured with about 5 seconds of residence time of water droplet on the surface.

Attenuated Total Reflection - Fourier Transform Infrared spectroscopy (ATR-FTIR) analysis was conducted in order to ascertain the current nature of any organic material present on the surfaces of the PDMS surfaces. ATR-FTIR scans were conducted using a Spotlight 400 (Perkin-Elmer, USA) from a wavelength of 700 to 4000 cm^{-1}. Reference spectra were taken from the Sigma library of FT-IR spectra and cross compared with the obtained spectra.

A Helios G4 CX DualBeam (FEI, USA) High resolution monochromated field emission gun scanning electron microscope (FEGSEM) with precise Focused Ion Beam (FIB) was used to determine the dry film thickness of the grafted surfaces. The microscope also facilitated energy dispersive x-ray spectroscopy (EDX) enabling elemental identification. Prior to FIB cross sectioning, samples were mounted, dehydrated in a light vacuum and coated with ~ 20 nm of iridium. Samples were then place in the microscope and a layer of platinum deposited via an electron and ion beam respectively. This was done to persevere surfaces during the argon ion beam FIB process. A 10 x 10 x 10 µm trench was milled to expose a cross-section of the interface. The cross sections were imaged under FEGSEM conditions to observe the film thickness. A minimum of two cross sections were made on each sample with two samples of each monomer variable being observed.

2.4. Tribological Evaluation

Tribological evaluation was conducted using a reciprocating NTR^3 tribometer (Figure 2, Anton Parr, Switzerland). The tribo-couple consisted of the PDMS-g-SPMK plate and borosilicate glass hemisphere probe (Ø = 15 mm). Friction forces were spatially resolved under piezo controlled actuation across a variety of loads and sliding speeds. This allowed the assessment of the load and velocity dependant frictional responses for the grafted surfaces. Frictional forces (F_t) as a function of load were characterised at normal loads (F_n) between 1 and 100 mN (for a total of 20 load increments) at a sliding speed of 500 µm/sec using a triangle wave displacement profile. In all studies, a sliding displacement (δ) of 500 µm was used. The speed dependence on F_t was also evaluated in this study under constant normal load conditions (F_n = 50 mN). The sliding speed was incrementally increased (total of 20 increments) from 0.01 – 10 mm/sec. Under all conditions, F_t was measured for a total of 50 cycles with a data acquisition rate of 400 Hz. The F_t vs δ loop was used to determine the average F_t per sliding cycle. This was taken as the average of the forward and reverse F_t under steady state, speed independent sliding conditions. 'Amonton's' coefficient of friction (μ_a) was determined from the gradient of F_t vs F_n curve according to Equation 2. The instantaneous coefficient of friction (i.e. $\mu_i = \frac{F_{tc}}{N_c}$ where F_{tc} and N_c are the tangential and normal load for a specific friction cycle 'c') was also calculated as a comparison. All tests were completed in triplicate under lubricated conditions consisting of 100 µL of de-ionised water or Phosphate Buffered Saline (PBS) solution. The results presented represent a mean of three samples with the associated standard deviation (n = 3 ± SD).

Eq2: $$F_t = \mu_a F_n + F_o$$

Where F_o is an unknown interfacial adhesion force.

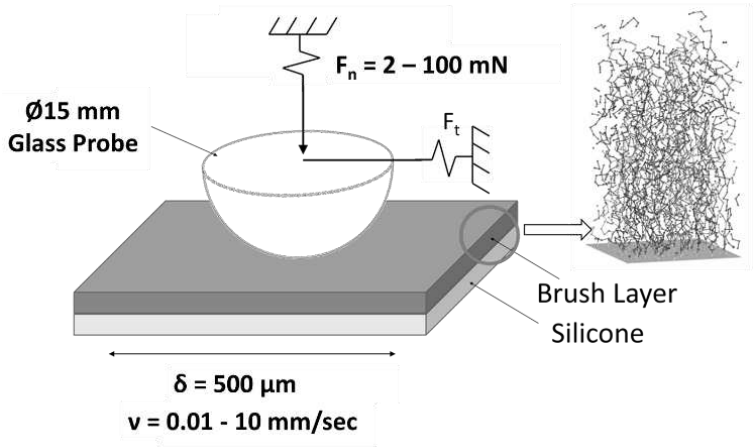

159

160 **Figure 2** – Schematic of tribological arrangement used in this study

161 **3. Results**

162

163 **3.1. Water Contact Angle (WCA) measurement**

164 Figure 3 shows examples of the obtained WCA for PDMS and the 20% PDMS-g-SPMK. A significant
165 reduction in the WCA was observed indicating an increased hydrophilicity, after the grafting process.
166 Table 1 lists the variation of WCA. A decrease from 89.85 to 19.50 ° in WCA was observed with
167 increasing monomer content.

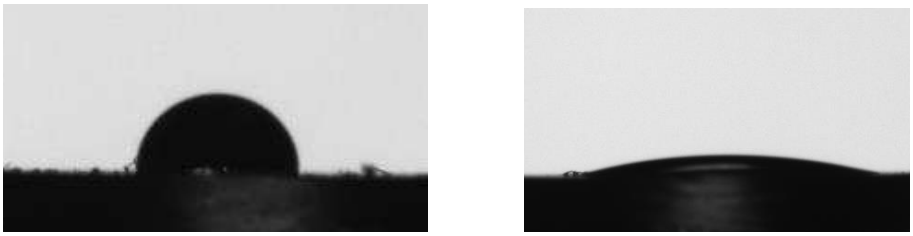

(a) **(b)**

168 **Figure 3 –** Example of WCA measurement for a) PDMS and b) 20% PDMS-g-SPMK after 3hrs UV
169 exposure. A significant reduction in the WCA was observed between samples.

170

171 **Table 1** – Water Contact Angle measurements (WCA) for PDMS and PDMS-g-SPMK

	WCA (°) ± SD
PDMS	89.85 ± 1.73
5% SPMK	23.06 ± 0.62
10% SPMK	20.09 ± 0.92
20% SPMK	19.50 ± 0.70

3.2. Fourier Transform Infrared Attenuated Total Reflectance Spectroscopy (FTIR - ATR)

Figure 4 shows the typical ATR-FTIR spectra obtained for PDMS and PDMS-g-SPMK surfaces. Differences in spectra was seen between un-grafted and grafted PDMS surfaces. No difference between grafted surfaces was seen. Table 2 summarises the peaks observed and their associated chemical bonding indicating the presence of SPMK on the surface. For the PDMS-g-SPMK surfaces, a adsorption peak at 1412 and 3373 cm^{-1} due to the water bound to the sulfonic acid groups of the SPMK was observed.

Table 2 – List of peak position observed on spectra presented in figure 4. Reference spectra were taken from the Sigma library of FT-IR spectra and cross compared with the obtained spectra.

	Peak position (cm^{-1})	**Functional group**
PDMS	2962	C-H, =C-H, - CH_2, -CH_3
	2905	C-H, O-H
	1285	Si-CH_3
	1014	Si-O-Si
	787	Si-CH_3
PDMS-g-SPMK	3720 – 3000	O-H, S-OH, S=O
	2962	C-H, =C-H, - CH_2, -CH_3
	2914	C-H,
	2858	-CH_2
	1722	C=O
	1640	C=C
	1412	S-O, S=O
	1258	Si-CH_3
	1014	Si-O-Si
	787	Si-CH_3

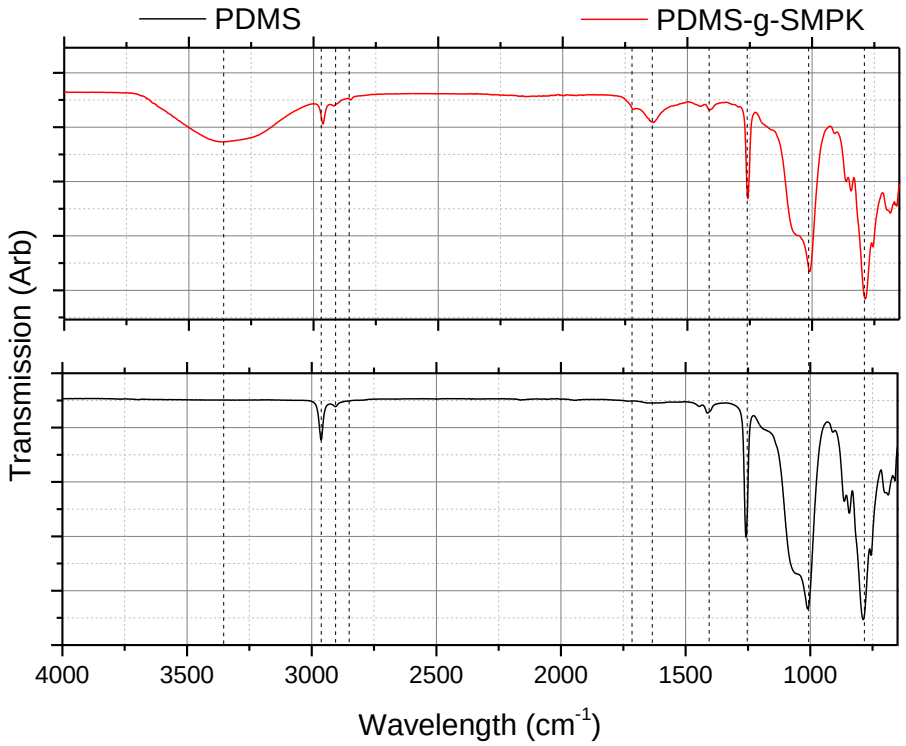

Figure 4 – FTIR-ATR Spectroscopy of un-grafted a) PDMS and b) PDMS-g-SPMK surfaces.

3.3. Focussed Ion Beam-Scanning Electron Microscopy

Figure 5 shows the cross-sectional FIB-SEM images of the dry grafted surfaces. Films of varying thickness were observed depending upon the initial monomer density, with thicker films observed with the higher initial monomer content. Due to charging of the sample, surfaces grafted with the lowest initial monomer content did not show evidence of a grafted film on the surface. Elemental EDX mapping of the interface demonstrated a concentration of sulphur at the PDMS interface further indicating the presence of a polymer SPMK layer. Dry film thicknesses in the region of 110 ± 53 and 1339 ± 148 nm were observed for initial monomer concentrations of 20 and 30 wt% SPMK. Table 3 lists the intrinsic viscosity and molecular weight of the polymer solutions after UV exposure.

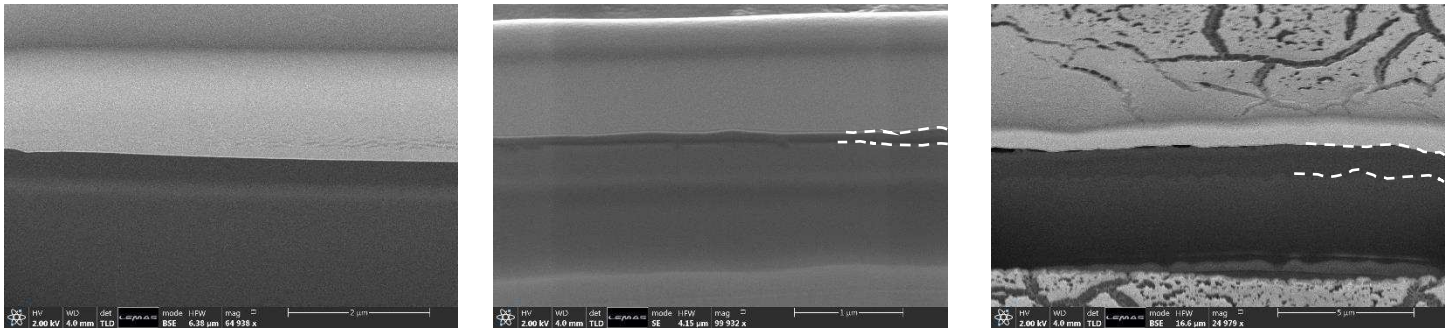

(a) **(b)** **(c)**

(d)

Figure 5 – FIB-SEM cross section images of films prepared with a) 10 b) 20 and c) 30 wt % SPMK solutions. Image d) shows elemental EDX mapping of the interface. Clear evidence of a polymer film was observed for surface grafted using 20 and 30 wt % initial monomer solutions, indicated by the white dashed lines.

Table 3 – intrinsic viscosity [η] and molecular weight (M_w) of polymer solutions after UV exposure. The molecular weight was calculated using Equation 1.

	wt% SPMK		
	5	**10**	**20**
[η]	0.05	0.40	0.83
M_n	477.19	37,709.80	163,907.00

3.4. Tribological Characterisation

Figure 6 shows an example of the raw data obtained during tribological evaluation. F_t traces were obtained, showing clear regions of steady state sliding under constant velocity. Figure 6b shows the F_t vs δ of which the average F_t per cycle was calculated (taken between ± 200 µm). Evidence of stick-slip transition was observed, highlighted in red on Figure 6b, which become more pronounced with increasing load.

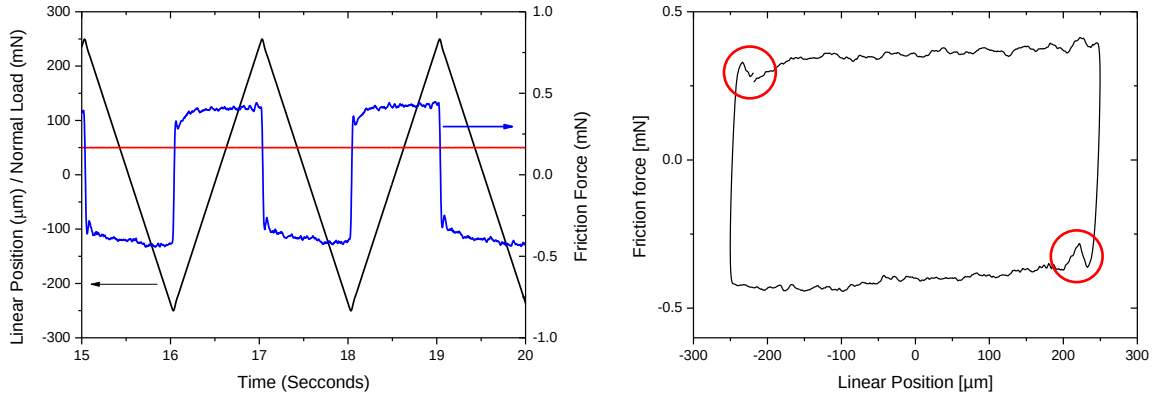

(a) **(b)**

208 **Figure 6** – Example of typical a) normal load (red), linear position (black) and tangential force (blue)
209 and b) friction force hysteresis loop at for 30 wt% PDMS-g-SPMK at F_n = 50 mN.

210 Figure 7 shows a representative example of instantaneous coefficient of friction as a function of time
211 for the PDMS, PDMS after 3hrs of UV exposure in the absence of monomer and PDMS-g-SPMK surfaces
212 lubricated with PBS at 50 mN. Over the 50 cycles μ_i was seen to be stable varying from 0.06 to 0.009
213 for the polymer functionalised surfaces depending on the initial monomer grafting concentration. No
214 significant difference in μ_i was seen as the load was increased incrementally for any of the monomer
215 concentrations tested. This was substantially lower than that observed for the as-cast PDMS and
216 PDMS subjected to plasma and UV exposure.

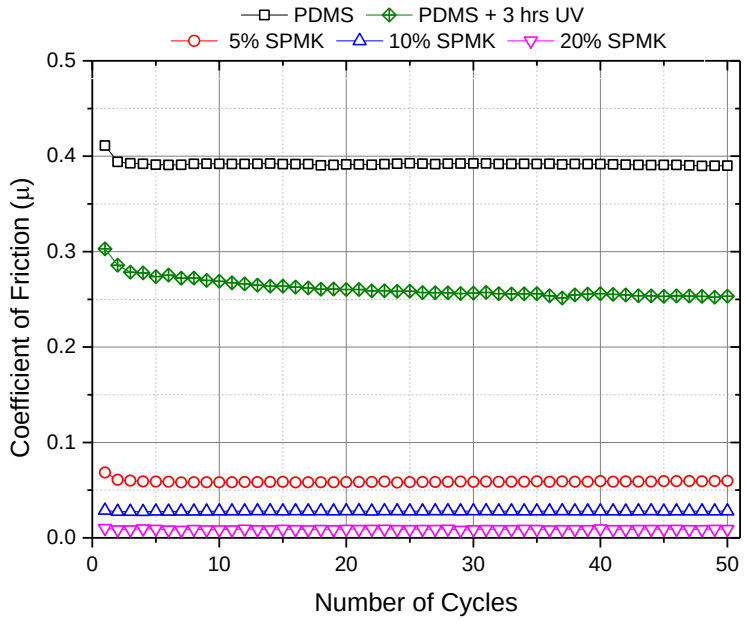

217

218 **Figure 7** - Representative instantaneous friction (μ_i) vs time for each loading time and monomer
219 content. The normal load (F_n) was at 50 mN

A comparative plot of F_t vs F_n, obtained according to the protocol outline in section 2, is shown in Figure 8. In all cases a near linear increase in F_t was observed with increasing F_n. A decrease in the coefficient of friction from $\mu_a = 0.382 \pm 0.03$ to 0.250 ± 0.04 was observed for surfaces subjected to plasma and UV exposure in the absence of monomer when compared to the as-cast PDMS surfaces. A substantial reduction in the coefficient of friction was observed for PDMS surfaces when exposed to UV in the presence of monomer. From Figure 8, it is evident that as M_i increases, a decrease in friction was observed. The average coefficient of friction calculated according to Eq 1 for the lowest M_i was $\mu_a = 0.117 \pm 0.06$. This was seen to further decrease to $\mu_a = 0.035 \pm 0.002$ and 0.009 ± 0.001 for PDMS-g-SPMK surfaces prepared using 10 and 20 wt% monomer solutions respectively. Frictional data demonstrates a significant decrease in friction when compared to un-functionalised silicone surfaces ($\mu_a = 0.382 \pm 0.03$).

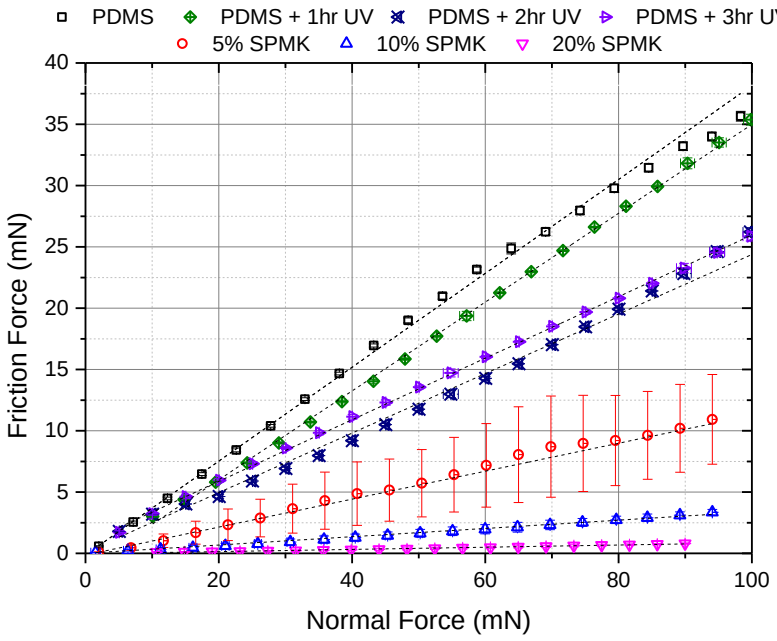

Figure 8 - Normal load vs friction force for different monomer content in PBS at 500 µm/sec

To investigate the role of the lubricant on friction, a small subset of experiments were carried out to investigate the presence of dissolved ions on the frictional properties of the PDMS-g-SPMK surfaces. In this case, the same tribological assessment was carried out as described above in de-ionised water for PDMS-g-SPMK surfaces prepared in 20 wt% monomer solution. Lower frictional forces were observed when lubricated with de-ionised water. The average coefficient of friction was $\mu_a = 0.009 \pm 0.001$ and 0.005 ± 0.001 for surfaces examined in PBS and de-ionised water respectively. Table 3 summarises the observed μ_a values in this study.

Table 3 – Average coefficient of friction for each monomer content and lubricant tested

	PDMS	PDMS + 1 hr UV	PDMS + 2 hr UV	PDMS + 3 hr UV	SPMK monomer content (wt %)		
					5%	10%	20%
PBS	0.382 ± 0.03	0.365 ± 0.02	0.255 ± 0.03	0.250 ± 0.09	0.120 ± 0.06	0.035 ± 0.002	0.009 ± 0.001
DI Water					-	-	0.005 ± 0.001

241

242 The speed dependant properties of the PDMS, PDMS after 3 hrs of UV exposure (PDMS + 3hrs UV) and
243 PDMS-g-SPMK surfaces were also assessed (Figure 9). For these experiments the coefficient of friction
244 was measured and averaged over the 50 cycles at a constant normal load of 50 mN. The plasma and
245 UV exposure steps was seen to reduce the coefficient of friction when compared to the as-cast PDMS.
246 However when compared to the PDMS surfaces prepared in the presence of monomer, a very
247 different response in the coefficient of friction was observed. Surfaces prepared with a lower M_i
248 content solutions demonstrated a more traditional speed dependence when compared to the surfaces
249 grafted with 20 wt% solutions, albeit at a much lower coefficient of friction when compared to
250 traditional lubricated engineering contacts. As M_i increased, a further reduction in the coefficient of
251 friction was observed.

252 For surfaces grafted in 5 wt% SPMK and lubricated in PBS, $\mu_i = 0.091 \pm 0.005$ at the lowest sliding speed
253 of 0.01 mm/sec. A transition in the coefficient of friction was observed as sliding speed increases.
254 Coefficient of friction reached a plateau at $\mu_i = 0.05 \pm 0.002$ at sliding speeds greater than 2 mm/sec.
255 As the initial monomer content increased, the coefficient of friction at lower sliding speeds also
256 decreased. At 0.01 mm/sec, $\mu_i = 0.064 \pm 0.001$ and 0.009 ± 0.001 for surfaces grafted in 10 and 20 w%
257 SPMK solutions respectively. For the surfaces grafted in 10 wt% SPMK, a similar decrease in coefficient
258 of friction was seen when compared to surfaces grafted with 5 wt% SPMK. However no plateau in the
259 coefficient of friction was observed with increasing sliding speed. Surfaces grafted with the highest
260 initial monomer content demonstrated a different speed dependant coefficient of friction response
261 when compared to the other two experiments. At 0.01 mm/sec, $\mu_i = 0.009 \pm 0.001$ which gradually
262 increased with sliding speed. At higher sliding speeds > 4 mm/sec, a rate change of coefficient of
263 friction was seen increasing to the power of 0.5 with respect to sliding speed.

264 The speed dependent coefficient of friction for PDMS-g-SPMK surfaces grafted in 20 wt% monomer
265 solutions were also studied in the absence of dissolved ions (i.e. de-ionised water). Figure 9 shows
266 that grafted surfaces tested in de-ionised water exhibited a lower coefficient when compared to those
267 in PBS; in line with results presented above. At 0.01 mm/sec, $\mu_i = 0.004 \pm 0.002$ which gradually
268 increased with sliding speed. At higher sliding speeds > 2 mm/sec, a rate change of coefficient of

friction was seen, increasing to the power of 0.5 with respect to sliding speed. The point in which this rate change was observed occurred earlier for surfaces lubricated with de-ionised water.

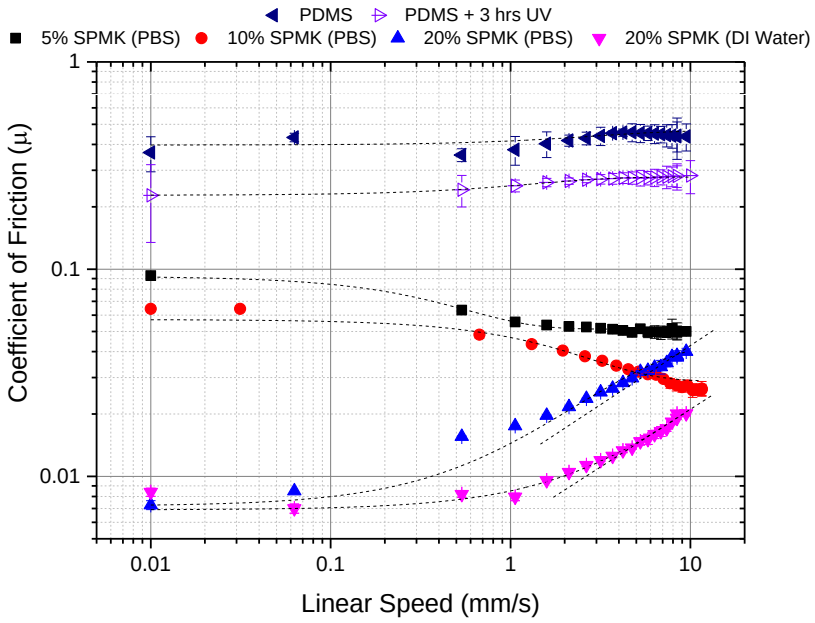

Figure 9 – Speed dependant friction for different monomer content at 50 mN

4. Discussion

This study has demonstrated the possibility to tailor the surface properties of silicone surfaces through a simple two stage grafting process. The results demonstrate the effectiveness of UV-enabled grafting of anionic polymers to an elastomer surface; enhancing wettability and frictional properties of the surfaces. Whilst exposure of the silicone surfaces to plasma and UV irradiation was seen to reduce the coefficient of friction, the reduction was not as significant when compared to the functionalised surfaces. The mechanisms pertaining to enhanced lubrication of PDMS after plasma treatment have been well documented [13]. However the roles of UV are not completely clear. A reduction in the coefficient of friction may arise from the combined increase in hydrophilicity and changes in mechanical properties and contact compliance as a result of further UV induced crosslinking of the PDMS surfaces. The results presented in this study also provide insight into the links between grafting variables, load bearing capacity and the roles of the environmental on friction. Some information regarding the films tenacity can also be inferred. Films demonstrated effective lubrication up to 500 mm of total sliding distance (20 increments of 25 mm total sliding distance at each load). This is well in excess of those expected during urinary catheterisation which would be in the region of 40 and 200 mm for female and males respectively. Modification of medical surfaces with hydrophilic polymer technologies has received considerable attention of the past years with the view to reduce friction and the occurrence of fouling [2, 5, 6, 14, 15]. However only a handful of researchers have investigated

the tribological properties of these layers and the mechanisms in which they impart lubricity. The work presented in this study shows the ability to create load bearing (within the context of medical devices) and lubricious surfaces; tuneable through the synthesis parameters. The coefficients of friction presented in this study are orders of magnitude lower than threshold acceptable values ($\mu < 0.3$) mooted by some researchers for catheterisation. SPMK brush surfaces have also been hypothesised to impart a certain degree of anti-fouling capability, which may be desirable for applications where adhesion of scale or proteins (in the case of urinary catheterisation) or blood cells may not be desirable [16]. The ability to produce lubricious and low fouling surfaces, without the addition of expensive heavy metals or additional therapeutics, presents a number of potential opportunities. The methods presented here are therefore considered to be a quick, easy and cost effective way for surface modification of silicone materials.

The grafting approach employed in this study aimed to create a layer of grafted polymers, or polymer brushes, utilising the ability of the SPMK and PDMS surface to undergo free radical polymerisation using UV irradiation. Assembly of such surface layers has been shown before both with or without the addition of photo-initiator [17-19]. However this approach exploited the covalent grafting of SPMK to the PDMS surface due to its charged nature and intended application. The hypothesised route of reaction for functionalization is given below (Figure 10). Initially, a UV source and O_3 are used to oxidise the C-H bonds available at the surface of PDMS. This technique is known to increase the water wettability of PDMS by virtue of creating –OH terminated surfaces on the upper layer on the polymer [20]. The 3-Sulfopropyl methacrylate potassium salt (SPMK) is then activated towards surface functionalization, again by using a UV source. This takes places as the exo- π (C=C) bond converts to the more stable endo- π bond. The 3-Sulfopropyl methacrylate potassium salt (SPMK) is then activated towards surface functionalization, again by using a UV source. This takes places as the exo- π (C=C) bond converts to the more stable endo- π bond. This form of alkene tautomerization enhanced by the presence of the electron withdrawing ester group on SPMK [21]. This generates a reactive carbocation species. These species have three bonds and hold a positive charge. Carbocations are unstable as they do not satisfy proper carbon valency [22]. These species are readily attacked by nucleophiles, such as hydroxyl or alcohol groups [23]. The species formed is also sterically unhindered, making attack in this conformation more likely. The newly created –OH groups on PDMS then react with the carbocation on SPMK. The oxygen's lone pair on PDMS attacks the carbocation. This creates an ether bond, C-O between the SPMK and the PDMS.

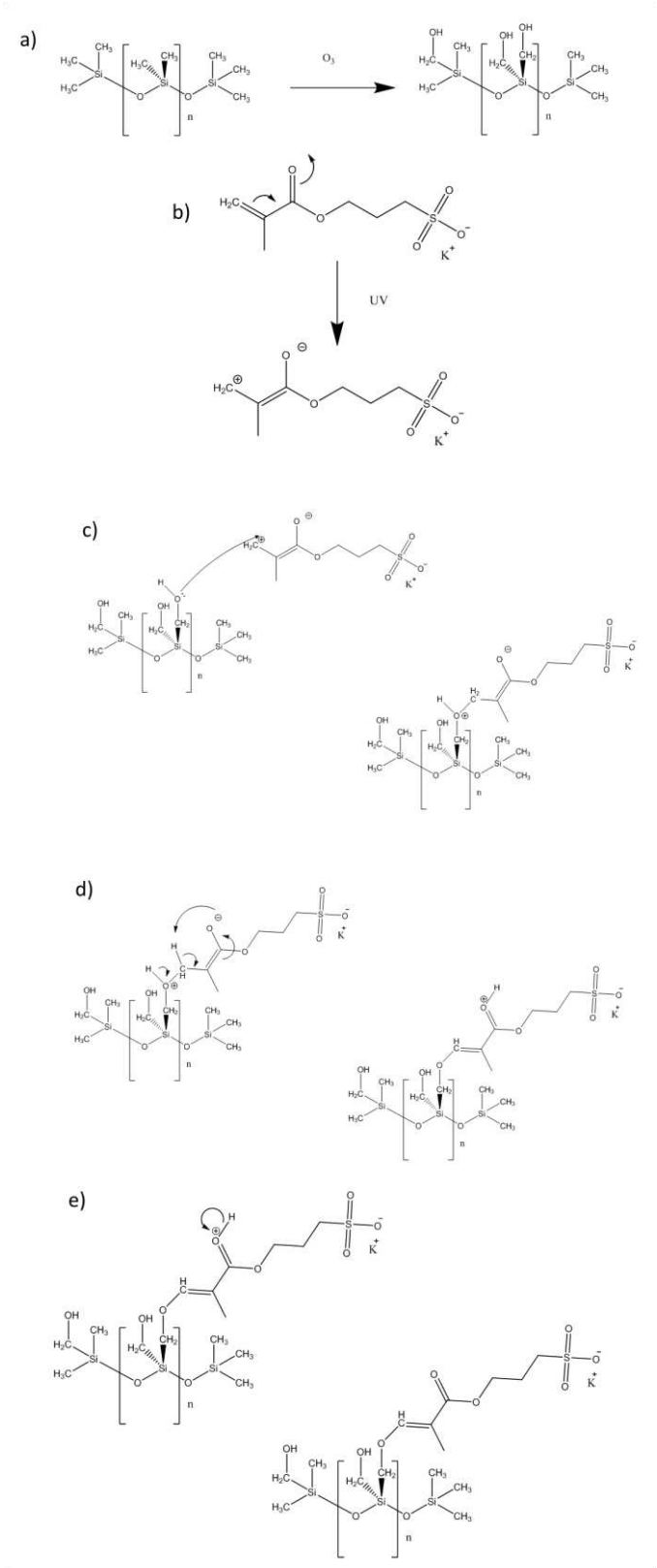

Figure 10 – Hypothesised schematic of a) hydroxylation of PDMS surface, b) UV activation of SPMK monomer, c) Attack of hydroxyl group from PDMS onto activated monomer, d) Reformation of the carbon π system and loss of a proton and e) Loss of the final proton to give a stable structure, with a conjugated π system.

Although difficult to conclusively prove, the proposed mechanism is the most feasible of the possible options. Hydroxylation of PDMS results in a surface that will attack electron deficient species. That is to say that, following standard chemical thermodynamics, the electron rich alcohol species is able to donate electrons into the electron deficient carbocation, thereby satisfying carbons normal bond valency and restoring normal carbon bonding [24]. The UV activation of SPMK would form such a product. The final product depicted contains a conjugated π system, imparting stability onto the molecule. Furthermore, this allows the possibility of the group to undergo further radical reactions. As a large portion of the PDMS surface will have been successfully hydroxylated, as demonstrated by an increase in water wettability, there are multiple points on which SPMK can attach to the surface. Therefore, it is highly likely that the PDMS surface has a series is SPMK molecules aligned along the upper layer. As the end group is charged, SPMK can align into a brush like structure. An example of the comb like polymer formed is given in Figure 11.

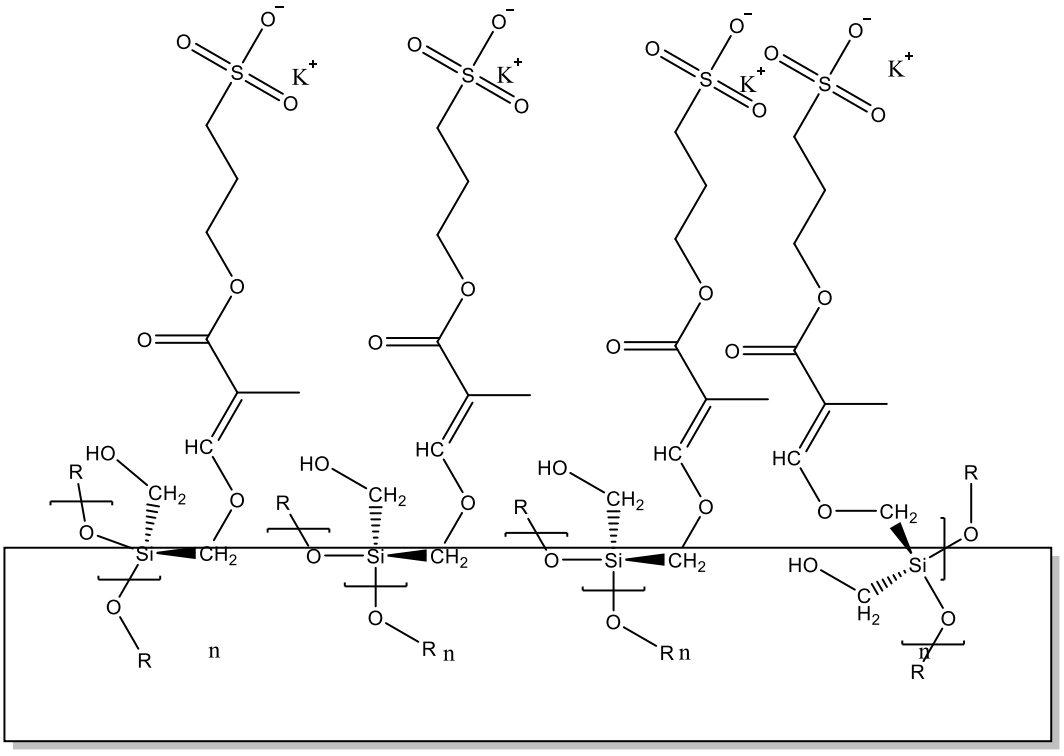

Figure 11 – Hypothesised polymer brush structure based on the materials used in this study

The frictional properties of grafted polymer layers have been well investigated and shown to be a function of graft time, monomer content and tribological environment [25]. Li et al [18] demonstrated the links between polymer grafting density, tuneable physicochemical properties and the links to frictional behaviour for polyacrylamide layers brush systems. They reported a linear increase in dry film thickness with UV exposure time; with the addition of cross-linker increasing the thickness of the films relative to surfaces with no cross-linker present. Interestingly, with increasing cross-linker

concentration within the films, a decrease in wettability and increase in friction was observed; signifying the importance of brush mediated lubrication and the role of brush terminated surfaces in frictional dissipation. Similar results have also been observed by other researchers with other polymer brush systems. Kyomoto et al [26] demonstrated that both initial polymer concentration and UV exposure time influences film thickness. This was attributable to the fact that the length of the polymer chains produced in a radical polymerization reaction correlates with initial monomer concentration and polymerisation time. A similar observation has been made in this study. Figure 5 shows that the dry film thickness (L) of the polymer layer increases with initial monomer content. It is apparent from Figure 5 and the estimation of the molecular weight after UV exposure that an increase in grafting density occurs with increasing monomer content. As a result, the polymer chains are more likely to be to a brush morphology as a result of a balance between an entropic effect, caused by higher orientation of the chains, and an energetic effect due to minimization of the repulsive interactions [27]. From the measurements presented here, it is difficult to estimate the correlation between thickness of the grafted layers and graft density due to the imaging limitations of the PDMS surfaces. Based on the thicknesses measured and the estimated molecular weight of the polymers after UV exposure (particularly for 10 and 20 wt% SPMK), the results presented here are in good agreement with the work of Ishihara and co-workers [10, 11, 17, 26], who have used similar approached to produce high molecular weight polymer brush functionalised surfaces. It must be noted that the molecular weight measured for the bulk fluid is known to deviate when compared to that of the surface tethered polymers [28].

The grafting procedure influences the mechanisms of friction and dissipation of shear at the interface. Whilst it is conceivable that lubricity may be achieved through a highly solvated low-modulus interface, the mechanisms in which this is achieved are complex, dependant on a number of factors including brush conformity. Although the full mechanisms behind brush mediated lubrication are not fully understood, the general consensus of opinion is that the hydrated brush architecture facilitates sliding and low friction through viscous dissipation of frictional forces [9, 29, 30]. Singh et al [31] demonstrated the effects of polymer stiffness and graft density on the hydration across the interface and resultant fictional characteristics using non equilibrium-molecular-dynamics. With the increase in grafting density, chains are more stretched out due to the excluded volume effect to support higher normal load and ensure a thin solvent layer at the interface. Similar predicted trends have been observed in this study with increasing graft density affecting both magnitude of friction and the speed dependant properties.

For surfaces prepared with 5 and 10 wt% SPMK solutions, the coefficient of friction was seen to display a ‘Stribeck –type’ transition. However it must be noted the magnitude of friction was much lower (μ

> 0.1) when compared to conventional 'boundary' lubricated engineering contacts (μ > 0.1). This variation may arise from the difference in conformity of the grafted brush layers (i.e. brush or mushroom), owing to the variable layer thickness and molecular weight of the polymers after UV exposure. The origins of friction in such systems has been hypothesised to arise from absorption-repulsion of polymer chains with the counter-surface and conventional soft elasto-hydrodynamic lubrication (sEHL) [32]. The former mechanism relies on absorption or repulsion of the polymer chains with respect to the counter-body; the magnitude of which is related to the kinetics of chain absorption – desorption. Although a speed dependent transition in the coefficient of friction was observed, this does not follow the 'absorption-repulsion' trends outlined by Kurokawa et al [32]. 20 wt% SPMK grafted surface demonstrated different friction-speed characteristics; the coefficient of friction was seen to remain constant up to ~ 1 mm/sec, with an increase being observed with increasing sliding speed (> 1 mm/sec). This was characterised by a rate change of coefficient of friction to the power of 0.5 with respect to sliding speed. Such a rate increase in friction can be predicted through soft elasto-hydrodynamic lubrication (sEHL) analysis. However care must be taken to appreciate the assumptions underpinning this model; prediction assumes linear elastic, iso-viscous, non-permeable surfaces with no lubricant-layer interactions. Pitenis et al [33] further hypothesised that such a rate increase in the coefficient of friction may arise from a 'relaxation lubrication' mechanism, whereby the resultant coefficient of friction is governed by the competing rates of polymer relaxation and sliding velocity. It must be noted that the hypotheses presented by these authors has been developed for covalently cross-linked hydrogel systems. Another difference relates to the substrate effects, contributing to overall contact modulus and depth dependant stiffness, which wouldn't be present in bulk gel systems.

Despite the recent work and seminal research by the aforementioned researchers, one aspect that is often neglected is the role of charge and the lubricant interactions at and within the interface. This consideration is of particular importance given the abundance of charged species *in-vivo* as well as the ability to produce and tailor net charged surfaces which are attractive from an anti-fouling point of view. Klein's [29] recently proposed hydration mechanism theory introduces these effects and their roles on hydrating and maintaining hydration at the interface. Klein's theory may explain these trends along with the velocity independent and dependant friction response observed in Figure 9. The decrease in layer thickness due to varying monomer content will not only affect the time dependant interfacial properties; the charge density and osmotic pressures at and within the interface will also vary. This will have an influence on the level of hydration at the interface and the ability of a surface to support a thin solvent layer at the interface facilitating low coefficient of friction at low sliding speeds and the transition into hydrodynamic lubrication regime. If a sEHL type mechanism exists at

the interface, it is conceivable that net fluid pressurisation required to separate the surfaces will vary depending upon the nature of grafted layer and chemistry of the lubricant (assuming a Newtonian lubricant). This would have the potential to promote or inhibit the transition to a hydrodynamic regime as seen in Figure 9. It also demonstrates further the short comings of this approach and application of this type of analysis to macromolecule mediated lubricated contacts. The presence of charge within the lubricant was also seen to influence friction. An increase in friction was observed when PBS was used when compared to de-ionised water. SPMK brush layers have been shown to be sensitive to the presence of cations and anions in solution, with the increasing salt concentrations affecting the brush conformation (i.e. collapsed) and an increase in coefficient of friction [34, 35]. An increase in salt concentration would lead to the reduction of the electrostatic repulsive interaction among the brushes resulting in a higher coefficient of efficient. The lubricant – brush interaction also influences the speed-dependant transition of the coefficient of friction. Considering the negligible differences in lubricant viscosity, the role of charge will likely influence their load bearing capacity by changing the brush conformation and as a result influencing the interfacial viscosity and contact mechanics. The use of PBS in these experiments represents a more complicated, but more realistic, situation in which cations and anions will be present at the interface further influencing osmotic processes at the interfaces. One aspect of further consideration will be the interactions with organic matter, such as proteins.

The results presented in this study demonstrate the ability to modify the surface of silicone elastomers through a simple three step method. There are a number of limiting factors that need to be considered. Whilst the lubricating ability of these films has been demonstrated, the contact pressures and contact areas in which they are subject to are unknown. Due to the thin film nature of these interfaces, the pressures within the films and substrate are difficult to predict using convention contact mechanics. Further work to understand the mechanics of soft thin film macroscopic contacts will be subject to further study. Whilst a gross-slip steady-state slip regime has been observed in Figure 6b, estimations of the contact area are difficult to make. Based on the range of mechanical values stated in literature, it is estimated that at least 90% of the contact emerges from original contact area during sliding. Evidence of a stick-slip transition was also observable. Further work to investigate the rehydration / dwell time at the contact, the fouling of these films, the influence of co-ion solutions on brush lubrication mechanisms, the durability of these layers and the effects of contact configuration including the frictional mechanisms against soft tissues.

5. Conclusions

This study has demonstrated an easy and effective method for grafting anionic polymer brushes to silicone surfaces. The influence of grafting variables has also been investigated, demonstrating clear links between monomer content and resultant frictional properties. The grafted surfaces prepared in this study are intended, but not limited to, for catheterisation devices where anti-fouling, anti-microbial and low friction are key. The load bearing capabilities of the layers have been demonstrated and testing under a wide range of loads. When slid against a glass probe, all PDMS-g-SPMK surfaces generated a coefficient of friction less than $\mu < 0.1$. At the highest initial monomer content $\mu < 0.01$ was achieved.

References

1 **Colas, A. and Curtis, J.** Silicone Biomaterials: History and Chemisrty In Ratner, B.H., A. Schoen, F. Lemons, J. , ed. *Biomaterials Science: An introduction to material in medicine* (Elsevier, USA, 2005).

2 **Brimelow, A.** Industry 'must do more' to improve urinary catheters. http://www.bbc.co.uk/news/health-33270030, 2015).

3 **Takashima, K., Shimomura, R., Kitou, T., Terada, H., Yoshinaka, K. and Ikeuchi, K.** Contact and friction between catheter and blood vessel. *Tribology International*, 2007, **40**(2), 319-328.

4 **Graiver, D., Durall, R.L. and Okada, T.** Surface morphology and friction coefficient of various types of Foley catheter. *Biomaterials*, 1993, **14**(6), 465-469.

5 **Mandakhalikar, K.D., Chua, R.R. and Tambyah, P.A.** New Technologies for Prevention of Catheter Associated Urinary Tract Infection. *Current Treatment Options in Infectious Diseases*, 2016, **8**(1), 24-41.

6 **Tunney, M.M. and Gorman, S.P.** Evaluation of a poly(vinyl pyrollidone)-coated biomaterial for urological use. *Biomaterials*, 2002, **23**(23), 4601-4608.

7 **Francois, P., Vaudaux, P., Nurdin, N., Mathieu, H.J., Descouts, P. and Lew, D.P.** Physical and biological effects of a surface coating procedure on polyurethane catheters. *Biomaterials*, 1996, **17**(7), 667-678.

8 **Mocny, P. and Klok, H.-A.** Tribology of surface-grafted polymer brushes. *Molecular Systems Design & Engineering*, 2016, **1**(2), 141-154.

9 **Lee, S. and Spencer, N.D.** Sweet, Hairy, Soft, and Slippery. *Science*, 2008, **319**(5863), 575-576.

10 **Kyomoto, M., Moro, T., Saiga, K., Hashimoto, M., Ito, H., Kawaguchi, H., Takatori, Y. and Ishihara, K.** Biomimetic hydration lubrication with various polyelectrolyte layers on cross-linked polyethylene orthopedic bearing materials. *Biomaterials*, 2012, **33**(18), 4451-4459.

11 **Ishihara, K.** Highly lubricated polymer interfaces for advanced artificial hip joints through biomimetic design. *Polym J*, 2015, **47**(9), 585-597.

12 **Lalani, R. and Liu, L.** Synthesis, characterization, and electrospinning of zwitterionic poly(sulfobetaine methacrylate). *Polymer*, 2011, **52**(23), 5344-5354.

13 **Bongaerts, J.H.H., Fourtouni, K. and Stokes, J.R.** Soft-tribology: Lubrication in a compliant PDMS–PDMS contact. *Tribology International*, 2007, **40**(10), 1531-1542.

14 **Rudy, A., Kuliasha, C., Uruena, J., Rex, J., Schulze, K.D., Stewart, D., Angelini, T., Sawyer, W.G. and Perry, S.S.** Lubricous Hydrogel Surface Coatings on Polydimethylsiloxane (PDMS). *Tribology Letters*, 2016, **65**(1), 3.

15 **Bermingham, S.L., Hodgkinson, S., Wright, S., Hayter, E., Spinks, J. and Pellowe, C.** *Intermittent self catheterisation with hydrophilic, gel reservoir, and non-coated catheters: a systematic review and cost effectiveness analysis*. 2013).

16 Higaki, Y., Kobayashi, M., Murakami, D. and Takahara, A. Anti-fouling behavior of polymer brush immobilized surfaces. *Polymer Journal*, 2016, **48**, 325.
17 Goda, T., Konno, T., Takai, M., Moro, T. and Ishihara, K. Biomimetic phosphorylcholine polymer grafting from polydimethylsiloxane surface using photo-induced polymerization. *Biomaterials*, 2006, **27**(30), 5151-5160.
18 Li, A., Benetti, E.M., Tranchida, D., Clasohm, J.N., Schönherr, H. and Spencer, N.D. Surface-Grafted, Covalently Cross-Linked Hydrogel Brushes with Tunable Interfacial and Bulk Properties. *Macromolecules*, 2011, **44**(13), 5344-5351.
19 Hu, S., Ren, X., Bachman, M., Sims, C.E., Li, G.P. and Allbritton, N. Surface Modification of Poly(dimethylsiloxane) Microfluidic Devices by Ultraviolet Polymer Grafting. *Analytical Chemistry*, 2002, **74**(16), 4117-4123.
20 Maji, D., Lahiri, S.K. and Das, S. Study of hydrophilicity and stability of chemically modified PDMS surface using piranha and KOH solution. *Surface and Interface Analysis*, 2012, **44**(1), 62-69.
21 Richard, J.P., Williams, G., O'Donoghu, A.C. and Amyes, T.L. Formation and Stability of Enolates of Acetamide and Acetate Anion: An Eigen Plot for Proton Transfer at α-Carbonyl Carbon. *Journal of the American Chemical Society*, 2002, **124**(12), 2957-2968.
22 Olah, G.A. Carbocations and Electrophilic Reactions. *Angewandte Chemie International Edition in English*, 1973, **12**(3), 173-212.
23 De La Mare, P.B.D. and Bolton, R. *Electrophilic Additions to Unsaturated Systems*. (Elsevier, 1966).
24 Ta-Shma, R. and Jencks, W.P. How does a reaction change its mechanism? General base catalysis of the addition of alcohols to 1-phenylethyl carbocations. *Journal of the American Chemical Society*, 1986, **108**(25), 8040-8050.
25 Wei, Q., Cai, M., Zhou, F. and Liu, W. Dramatically Tuning Friction Using Responsive Polyelectrolyte Brushes. *Macromolecules*, 2013, **46**(23), 9368-9379.
26 Kyomoto, M., Moro, T., Miyaji, F., Hashimoto, M., Kawaguchi, H., Takatori, Y., Nakamura, K. and Ishihara, K. Effect of 2-methacryloyloxyethyl phosphorylcholine concentration on photo-induced graft polymerization of polyethylene in reducing the wear of orthopaedic bearing surface. *Journal of Biomedical Materials Research Part A*, 2008, **86A**(2), 439-447.
27 Advincula, R., Brittain, W., C. Caster, K. and Rühe, J. *Polymer Brushes: Synthesis, Characterization, Applications*. 2004).
28 Kang, C., Crockett, R.M. and Spencer, N.D. Molecular-Weight Determination of Polymer Brushes Generated by SI-ATRP on Flat Surfaces. *Macromolecules*, 2014, **47**(1), 269-275.
29 Klein, J. Hydration lubrication. *Friction*, 2013, **1**(1), 1-23.
30 Tadmor, R., Janik, J., Klein, J. and Fetters, L.J. Sliding Friction with Polymer Brushes. *Physical Review Letters*, 2003, **91**(11), 115503.
31 Singh, M., Ilg, P., Espinosa-Marzal, R., Spencer, N. and Kröger, M. Influence of Chain Stiffness, Grafting Density and Normal Load on the Tribological and Structural Behavior of Polymer Brushes: A Nonequilibrium-Molecular-Dynamics Study. *Polymers*, 2016, **8**(7), 254.
32 Kurokawa, T., Tominaga, T., Katsuyama, Y., Kuwabara, R., Furukawa, H., Osada, Y. and Gong, J.P. Elastic−Hydrodynamic Transition of Gel Friction. *Langmuir*, 2005, **21**(19), 8643-8648.
33 Pitenis, A.A., Uruena, J.M., Schulze, K.D., Nixon, R.M., Dunn, A.C., Krick, B.A., Sawyer, W.G. and Angelini, T.E. Polymer fluctuation lubrication in hydrogel gemini interfaces. *Soft Matter*, 2014, **10**(44), 8955-8962.
34 Motoyasu, K. and Atsushi, T. Tribological properties of hydrophilic polymer brushes under wet conditions. *The Chemical Record*, 2010, **10**(4), 208-216.
35 Xiao, S., Ren, B., Huang, L., Shen, M., Zhang, Y., Zhong, M., Yang, J. and Zheng, J. Salt-responsive zwitterionic polymer brushes with anti-polyelectrolyte property. *Current Opinion in Chemical Engineering*, 2018, **19**, 86-93.